

Equivalent forces for colliding ocean waves

Toshiro Tanimoto

Department of Earth Science, University of California, Santa Barbara, CA 93106, USA. E-mail: toshiro@geol.ucsb.edu

Accepted 2010 January 4. Received 2010 January 4; in original form 2009 December 29

SUMMARY

Colliding ocean waves is considered to be the major source of seismic noise. In this paper, we examine the question, what would be the equivalent forces for such colliding ocean waves? In addition to the vertical pressure force term pointed out by Longuet-Higgins, we find that a lateral pressure gradient term is included in this system. This leads to a lateral dipole force and the excitation of noise that is different from vertical forcing. Numerical evaluation with PREM-like models shows that this term may become more important than vertical pressure term for frequencies below 5 millihertz (mHz). Importance of this horizontal term at low frequencies is related to the fact that horizontal motions of ocean waves become dominant in the low frequency band and its square is proportional to the excitation.

Key words: Non-linear differential equations; Surface waves and free oscillations; Theoretical seismology; Wave propagation.

1 INTRODUCTION

For the mechanism of seismic noise excitation by ocean waves, two papers have had the dominant influence in our thinking: Longuet-Higgins (1950) and Hasselman (1963). Longuet-Higgins (1950) showed that colliding ocean waves generate deep-penetrating pressure variations through the non-linear term in the Navier–Stokes equation, even though ocean waves may be confined to shallow depths in the ocean. This mechanism successfully explained the double-frequency peak in seismic noise (microseisms) at about 0.15 Hz, the most prominent seismic noise in the entire seismic frequency band (0.001–10 Hz). In this paper, we refer to this mechanism as the Longuet-Higgins mechanism.

Hasselman (1963) formulated his theory for a more general wavefield that included wide range of wavenumbers and frequencies and showed how opposing waves make the dominant contributions, thus lending support for the Longuet-Higgins mechanism. An important aspect of this paper was that the randomness in ocean waves was included in the analysis which was not in Longuet-Higgins (1950). Randomness is an important property of ocean waves, as winds can constantly generate small-scale ocean waves through atmosphere–ocean coupling at ocean surface.

These papers examined pressure fluctuation generated by ocean waves as pressure fluctuation works as a vertical force on the ocean floor which then excites seismic noise in the solid earth. One can formulate this excitation problem by skipping this pressure fluctuation, however; one can directly treat ocean waves as the excitation source of seismic noise and write down formulas for seismic wavefields generated by them. In Tanimoto (2007), hereafter referred as Paper I, we did this by using the normal mode theory formulation and analysing excitation of Earth's normal modes by the non-linear interaction of ocean waves. The theory accounts for all terms up to the second order in ocean-wave amplitudes. We will maintain the same level of approximation in this paper.

One of the surprises in Paper I was the existence of horizontal forcing term in addition to pressure perturbation related to the Longuet-Higgins mechanism. The same term was also noted by Webb (2007, 2008) in his extension of Hasselman's formulation, although the origin of this term was not clear. The main purpose of this paper is to clarify the source of this term and examine its effects within the framework of our normal-mode excitation theory.

In this paper, we drop the randomness in ocean waves and ask a rather idealized question: what is the equivalent force for colliding ocean waves? We believe that basic physical forcing terms arise in this idealized situation, although the inclusion of randomness may be essential for data modelling.

In Section 2, we point out the existence of horizontal pressure gradient in the field of colliding ocean waves, through non-linear interaction among them. In Section 3, we will show that the same term arises in the normal-mode formula, derived in Paper I, whose effect can be interpreted as a horizontal dipole force near the surface. We will discuss some characteristics of this dipole in Sections 4 and 5 including its numerical evaluation. Conclusion will be in Section 6. Some details in lengthy derivations are given in the Appendix to clarify the algebraic steps.

2 LATERAL PRESSURE GRADIENT

In this section, we will show that, in the presence of colliding ocean surface waves, lateral pressure gradient is generated in addition to pressure perturbation. We will analyse the momentum equation for the ocean (perfect fluid here) to get physical insight into this problem.

2.1 Momentum equation

The equations of motion in the ocean can be written

$$\rho \frac{\partial v_i}{\partial t} + \rho \left(v_j \frac{\partial}{\partial x_j} \right) v_i = - \frac{\partial p}{\partial x_i} - \rho g \delta_{iz} \quad (1)$$

assuming that this layer consists of non-viscous fluid. This is written in the Cartesian form, and the indices i and j are x , y or z , respectively. The summation convention for a repeated index is assumed. We take the x - and y -axes in the horizontal plane and the z -axis vertically (positive upward). Gravitational acceleration is g and δ_{iz} is the Kronecker's delta.

We analysed the vertical momentum equation in Paper I, using an approach similar to Phillips (1977). Our focus in this paper is lateral forcing and thus we examine equations for x - and y -components. We define the ocean bottom by $z = -d$ and the ocean surface by $z = \zeta(x, y, t)$, where $\zeta(x, y, t)$ changes with time and space, although its spatial average is zero ($\bar{\zeta} = 0$). In the absence of ocean waves, the ocean surface is at $z = 0$. Writing three (x , y and z) components of velocity as (u, v, w) , we can write two horizontal momentum equations as

$$\rho \frac{\partial u}{\partial t} + \rho \left(u \frac{\partial u}{\partial x} + v \frac{\partial u}{\partial y} + w \frac{\partial u}{\partial z} \right) = - \frac{\partial p}{\partial x} \quad (2)$$

$$\rho \frac{\partial v}{\partial t} + \rho \left(u \frac{\partial v}{\partial x} + v \frac{\partial v}{\partial y} + w \frac{\partial v}{\partial z} \right) = - \frac{\partial p}{\partial y}. \quad (3)$$

For simplicity, we assume that density (ρ) is constant.

By integrating (2) and (3) over the oceanic layer, we get

$$- \int_{-d}^{\zeta} \frac{\partial p}{\partial x} dz = \rho \int_{-d}^{\zeta} \frac{\partial u}{\partial t} dz + \rho \int_{-d}^{\zeta} \left(u \frac{\partial u}{\partial x} + v \frac{\partial u}{\partial y} + w \frac{\partial u}{\partial z} \right) dz \quad (4)$$

$$- \int_{-d}^{\zeta} \frac{\partial p}{\partial y} dz = \rho \int_{-d}^{\zeta} \frac{\partial v}{\partial t} dz + \rho \int_{-d}^{\zeta} \left(u \frac{\partial v}{\partial x} + v \frac{\partial v}{\partial y} + w \frac{\partial v}{\partial z} \right) dz. \quad (5)$$

2.2 Formulas for ocean waves

To analyse the eqs (4) and (5), we will use analytical formulas for ocean waves. These were given in Paper I but for completeness, we summarize the formulas below.

When ocean waves are present, vertical ocean-surface displacement can be written by a superposition of linear waves as

$$\begin{aligned} \zeta(x, y, t) &= \int dk_x \int dk_y a(k_x, k_y) \sin(\omega t - k_x x - k_y y) \\ &\equiv \int d\mathbf{k} a(\mathbf{k}) \sin(\omega t - \mathbf{k} \cdot \mathbf{x}), \end{aligned} \quad (6)$$

where a is the amplitude, ω is the angular frequency and \mathbf{k} is the horizontal wavenumber whose x - and y -components are (k_x, k_y) . For the frequency range of interest (0.001–0.5 Hz), gravity is the dominant restoring force for ocean waves. The dispersion relation for gravity waves is given by

$$\omega^2 = gk \tanh(kd), \quad (7)$$

where $k = |\mathbf{k}|$.

Velocity wavefields of linear ocean waves can be written as

$$(w, u, v) = \int d\mathbf{k} a(\mathbf{k}) \vec{\xi}(\mathbf{k}), \quad (8)$$

where $\vec{\xi}(\mathbf{k}) = [\xi_z(\mathbf{k}), \xi_x(\mathbf{k}), \xi_y(\mathbf{k})]$ with

$$\xi_z(\mathbf{k}) = A_k \cos(\omega t - k_x x - k_y y),$$

$$\xi_x(\mathbf{k}) = B_k \frac{k_x}{k} \sin(\omega t - k_x x - k_y y),$$

$$\xi_y(\mathbf{k}) = B_k \frac{k_y}{k} \sin(\omega t - k_x x - k_y y). \quad (9)$$

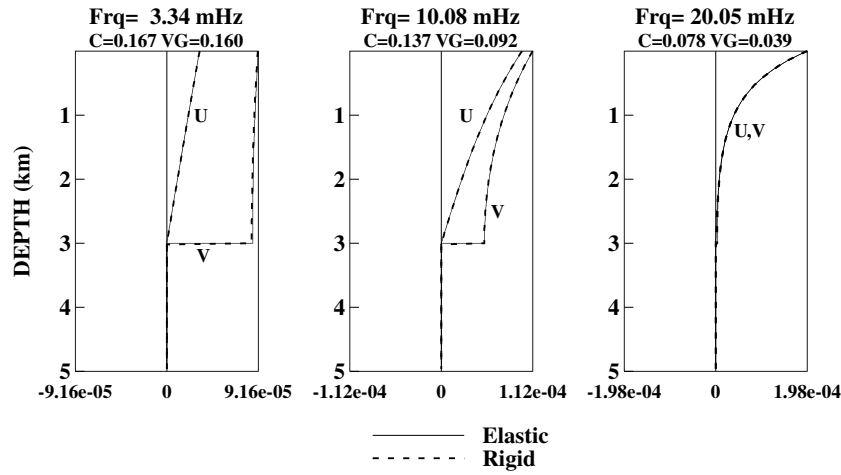


Figure 1. Comparison of eigenfunctions between analytical, rigid-bottom solutions (dash) and numerically derived ocean-wave (tsunami) modes (solid). PREM was used for numerical evaluation. In low frequency bands, horizontal eigenfunction V become much larger than vertical eigenfunction U as the left-hand figure (3.34 mHz) shows.

Here we used the order of components in the order z -, x - and y -components and defined

$$A_k = \frac{\omega \sinh\{k(z + d)\}}{\sinh(kd)}, \tag{10}$$

$$B_k = \frac{\omega \cosh\{k(z + d)\}}{\sinh(kd)}. \tag{11}$$

We use these analytical formulas when evaluating the excitation terms for seismic noise. These are approximations but are good approximations as Fig. 1 shows. This figure compares the above solutions (dash) against numerically derived ocean-wave modes that were computed for the model PREM (Dziewonski & Anderson 1981). The oceanic layer (top 3 km) is underlain by elastic medium in PREM while the rigid boundary condition was assumed at ocean bottom for the above analytical solutions. The vertical eigenfunction is U and the horizontal eigenfunction is V in the figure and both agree quite well.

Strictly speaking, there are up to a percent deviation between the two solutions but the main physics of the problem should be recovered by the use of these approximate analytical solutions.

2.3 Level of approximation

To clarify the assumptions and the level of approximations in the following analysis, we take a simple example from surface displacement and describe our approach; surface displacement can be written as

$$\zeta(\mathbf{x}) = \int d\mathbf{k}' a(\mathbf{k}') \sin(\omega't - \mathbf{k}' \cdot \mathbf{x}), \tag{12}$$

where it contains multiple wavenumbers.

The guiding principles in the analysis are two-fold: (1) ocean waves may be large, in comparison to elastic waves in solid earth, and thus we will keep terms beyond linear terms, up to the order $O(a^2)$. In solid media, only linear terms are kept. It is important to realize that there are only two sources of non-linearity in this problem. One is the advection term in the Navier–Stokes equation and the other is the kinematic boundary condition at ocean surface. We will analyse these non-linear terms fully, up to the second-order $O(a^2)$. (2) Spatial average will be taken, which means only averaged quantities are examined. This is the same with Longuet-Higgins (1950) and leads to elimination of terms of order $O(a)$.

As an example, let us analyse the square of ζ , vertical displacement of ocean surface; it can be written by a double integral as

$$\begin{aligned} \zeta^2 &= \int d\mathbf{k}' \int d\mathbf{k}'' a(\mathbf{k}') a(\mathbf{k}'') \sin(\omega't - \mathbf{k}' \cdot \mathbf{x}) \sin(\omega''t - \mathbf{k}'' \cdot \mathbf{x}) \\ &= \frac{1}{2} \int d\mathbf{k}' \int d\mathbf{k}'' a(\mathbf{k}') a(\mathbf{k}'') \\ &\quad \times [\cos\{(\omega' - \omega'')t - (\mathbf{k}' - \mathbf{k}'') \cdot \mathbf{x}\} - \cos\{(\omega' + \omega'')t - (\mathbf{k}' + \mathbf{k}'') \cdot \mathbf{x}\}]. \end{aligned} \tag{13}$$

Pairs of frequency and wavenumber (ω', \mathbf{k}') and (ω'', \mathbf{k}'') satisfy the dispersion relation in (7), respectively.

We now consider spatial averaging of this quantity, ζ^2 , over a source area defined by $L_x \times L_y$ where L_x and L_y are the length scales of source in the x - and y -directions. The most critical assumption we make is $L_x, L_y \gg \lambda$ where λ is the wavelength of ocean waves corresponding

to the above wavenumbers. The wavelengths of ocean waves at a period of 7 s is about $\lambda \approx 80$ m, where 7 s is the period of the most dominant seismic noise. If $L_x, L_y \approx 1$ km, this assumption is well justified. While we are not sure if this is always justified, it seems to be a good assumption in winter when ocean waves are typically quite high over large areas. When this condition is satisfied, we have, for example for a 1-D integral,

$$\frac{1}{L} \int_0^L \cos\{(k' - k'')x\} dx \rightarrow \delta_{k'k''} \quad (14)$$

as L becomes large.

If we apply similar approximations to (13), a 2-D case, we get

$$\overline{\xi^2} = \frac{L_x L_y}{2} \int d\mathbf{k}' \{a(\mathbf{k}')^2 + a(\mathbf{k}')a(-\mathbf{k}') \cos(2\omega't)\} \quad (15)$$

as the main contribution occur when $\mathbf{k}' = \mathbf{k}''$ or $\mathbf{k}' = -\mathbf{k}''$, both with $\omega' = \omega''$. Therefore, the dominant term in $\overline{\xi^2}$ is the static term and the double-frequency term at frequency $2\omega'$.

Similar analysis will be applied to all terms that arise in the following analysis.

2.4 Lateral pressure gradient terms

We now analyse (4) and (5) by the approach described in 2.3. Substitution of (8)–(11) on the right-hand side of (4), performing z integration and keeping up to terms of order $O(a^2)$ leads us to

$$\overline{\rho \int_{-d}^{\xi} \frac{\partial u}{\partial t} dz} = \int d\mathbf{k}' \frac{\rho g k'_x}{2} a(\mathbf{k}')a(-\mathbf{k}') \sin(2\omega't) \quad (16)$$

and

$$\overline{\rho \int_{-d}^{\xi} \left(u \frac{\partial u}{\partial x} + v \frac{\partial u}{\partial y} + w \frac{\partial u}{\partial z} \right) dz} = \int d\mathbf{k}' \frac{\rho g k'_x}{2} a(\mathbf{k}')a(-\mathbf{k}') \sin(2\omega't). \quad (17)$$

We provide the details of derivation for (16) and (17) in the Appendix.

We then have from (4)

$$-\overline{\Delta P_x} \equiv -\overline{\int_{-d}^{\xi} \frac{\partial p}{\partial x} dz} = \int d\mathbf{k}' \rho g k'_x a(\mathbf{k}')a(-\mathbf{k}') \sin(2\omega't). \quad (18)$$

By performing similar analysis on (5), we get

$$-\overline{\Delta P_y} \equiv -\overline{\int_{-d}^{\xi} \frac{\partial p}{\partial y} dz} = \int d\mathbf{k}' \rho g k'_y a(\mathbf{k}')a(-\mathbf{k}') \sin(2\omega't). \quad (19)$$

These are the lateral pressure gradient generated by colliding ocean waves. Both $\overline{\Delta P_x}$ and $\overline{\Delta P_y}$ are integrated quantity over the depth of ocean. Note that the pressure gradient term in the x -direction in (18) contains k'_x and that in the y -direction in (19) contains k'_y . If the direction of ocean-wave collision is oblique, the wavenumber in that particular direction will simply be obtained by replacing k'_x or k'_y .

In Paper I, we derived a similar expression for the vertical component

$$-\overline{\Delta P_z} \equiv \int d\mathbf{k}' \rho \omega'^2 a(\mathbf{k}')a(-\mathbf{k}') \cos(2\omega't). \quad (20)$$

For the vertical (z) component, we also get a hydrostatic pressure term ($\rho g d$) but this term is the zero-frequency static term. The time varying dynamic part is the term on the right-hand side of (20). In Paper I, we showed that this term is equal to the Longuet-Higgins pressure term (Longuet-Higgins 1950). We thus refer to this as P_L in place of $-\overline{\Delta P_z}$ in later sections.

The main purpose of defining three quantities, $\overline{\Delta P_x}$, $\overline{\Delta P_y}$, and P_L , is that they can be identified in the normal-mode excitation formula in Section 4. The first two are horizontal dipoles and the third is vertical force.

3 NORMAL MODE SOLUTION

Using ocean waves as the direct forcing term, we derived normal-mode solutions in Paper I. Displacement formulas for the vertical and horizontal components derived in Paper I were (Tanimoto 2007, eq. 38)

$$u_z(t) = \frac{L_x L_y}{4\pi^2} \int_{-\infty}^{\infty} d\mathbf{k} U(\mathbf{k}) \int_{-\infty}^t d\tau \frac{\sin \omega(t - \tau)}{\omega} \int_{-\infty}^{\infty} d\mathbf{k}' a(\mathbf{k}')a(-\mathbf{k}') \times \{-C_Z \cos(2\omega'\tau) \cos(\mathbf{k} \cdot \mathbf{x}) + C_H \cos \Psi \sin(2\omega'\tau) \sin(\mathbf{k} \cdot \mathbf{x})\} \quad (21)$$

$$u_x(t) = \frac{L_x L_y}{4\pi^2} \int_{-\infty}^{\infty} d\mathbf{k} V(\mathbf{k}) \int_{-\infty}^t d\tau \frac{\sin \omega(t - \tau)}{\omega} \int_{-\infty}^{\infty} d\mathbf{k}' a(\mathbf{k}')a(-\mathbf{k}') \times \frac{k_x}{k} \{C_Z \cos(2\omega'\tau) \sin(\mathbf{k} \cdot \mathbf{x}) + C_H \cos \Psi \sin(2\omega'\tau) \cos(\mathbf{k} \cdot \mathbf{x})\} \quad (22)$$

$$u_y(t) = \frac{L_x L_y}{4\pi^2} \int_{-\infty}^{\infty} d\mathbf{k} V(\mathbf{k}) \int_{-\infty}^t d\tau \frac{\sin \omega(t - \tau)}{\omega} \int_{-\infty}^{\infty} d\mathbf{k}' a(\mathbf{k}') a(-\mathbf{k}') \times \frac{k_y}{k} \{C_Z \cos(2\omega' \tau) \sin(\mathbf{k} \cdot \mathbf{x}) + C_H \cos \Psi \sin(2\omega' \tau) \cos(\mathbf{k} \cdot \mathbf{x})\}. \tag{23}$$

In these formulas, U and V are vertical and horizontal eigenfunctions of Rayleigh waves for the wavenumber k ($=|\mathbf{k}|$). The wavenumbers for seismic waves are without primes and those for ocean waves have the primes. The integration over \mathbf{k}' exists because ocean wave collisions from various directions and wavenumbers are included. The convolution integral over time (τ) exists because all noise sources before the current time t are included. The term $a(\mathbf{k}') a(-\mathbf{k}')$ indicates multiplication of amplitudes for opposing ocean waves. Two coefficients C_Z and C_H are defined by

$$C_Z = \frac{\rho \omega'^2 U(0)}{2} + \int_{-d}^0 \rho U(z) A_{k'} B_{k'} k' dz \tag{24}$$

$$C_H = \frac{\rho g k' V(0)}{2} + \int_{-d}^0 \rho V(z) \frac{A_{k'}^2 + B_{k'}^2}{2} k' dz, \tag{25}$$

where $A_{k'}$ and $B_{k'}$ are given in (10) and (11).

C_Z is related to pressure force term in the Longuet-Higgins mechanism and C_H is related to the horizontal dipole generated from lateral pressure gradient. In both cases, the first terms on the right-hand side of (24) and (25) arise from the surface boundary condition for ocean waves and the second from the non-linear (advection) term in the Navier–Stokes equation.

4 PHYSICAL MEANING

Let us now consider a single pair of colliding ocean waves, dropping the \mathbf{k}' integral from (21) to (23), as it becomes easy to understand physical meaning of various terms. There is no loss of generality in assuming that the direction of \mathbf{k}' (ocean wave collision) is the x -direction (Fig. 2). Then Rayleigh-wave propagation angle Ψ is defined as in Fig. 2. If we write the formulas for Rayleigh waves in the direction Ψ , noting that the wavenumbers in this case become $k_x = k \cos \Psi$ and $k_y = k \sin \Psi$, we get for the vertical component

$$u_z(t) = \frac{L_x L_y}{4\pi^2} \int_{-\infty}^{\infty} d\mathbf{k} U(\mathbf{k}) \int_{-\infty}^t d\tau \frac{\sin \omega(t - \tau)}{\omega} a(\mathbf{k}') a(-\mathbf{k}') \times \{-C_Z \cos(2\omega' \tau) \cos(\mathbf{k} \cdot \mathbf{x}) + C_H \cos \Psi \sin(2\omega' \tau) \sin(\mathbf{k} \cdot \mathbf{x})\}, \tag{26}$$

for the radial component

$$u_r(t) = u_x \cos \Psi + u_y \sin \Psi = \frac{L_x L_y}{4\pi^2} \int_{-\infty}^{\infty} d\mathbf{k} V(\mathbf{k}) \int_{-\infty}^t d\tau \frac{\sin \omega(t - \tau)}{\omega} a(\mathbf{k}') a(-\mathbf{k}') \times \{C_Z \cos(2\omega' \tau) \sin(\mathbf{k} \cdot \mathbf{x}) + C_H \cos \Psi \sin(2\omega' \tau) \cos(\mathbf{k} \cdot \mathbf{x})\}, \tag{27}$$

and for the transverse component

$$u_t(t) = -u_x \sin \Psi + u_y \cos \Psi = 0.$$

The transverse component vanishes. This result is important as toroidal-mode hum (Kurrle & Widmer-Schmidrig 2008) and Love waves in seismic noise are now commonly observed. It shows that colliding ocean waves alone cannot possibly explain such observations.

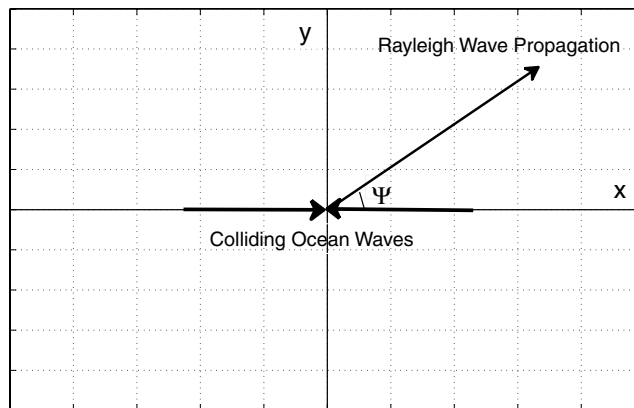


Figure 2. Direction of ocean wave collision is taken as the x -axis. Direction of wave propagation is at an angle Ψ from it. Excitation by dipole terms contain the term $\cos \Psi$ as the radiation pattern for Rayleigh waves.

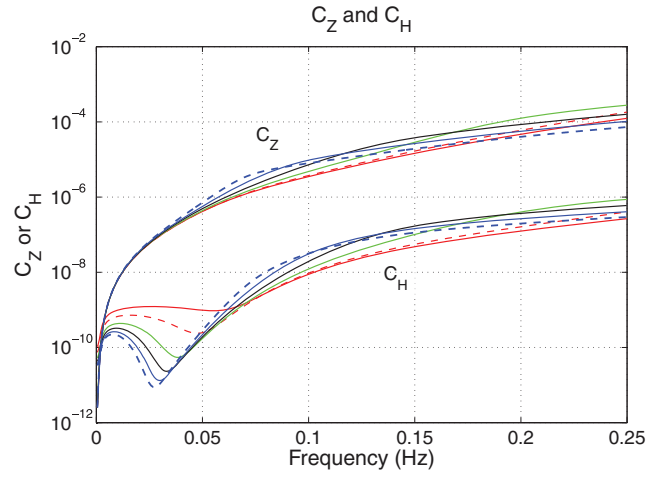


Figure 3. Numerical evaluation of C_Z and C_H . PREM-like models with six different ocean depths are shown. Colours correspond to ocean depths 0.5 km (red solid), 1 km (red dash), 2 km (green), 3 km (black), 4 km (blue solid) and 5 km (blue dash).

4.1 Low frequency limit

Toward lower frequency limit, eigenfunctions of Rayleigh waves approach to constant values within the oceanic layer as the eigenfunctions penetrate to a few hundred to a thousand kilometres whereas the oceanic layer is a thin, near-surface layer with thickness less than 10 km. In such a case, the integrations in (24) and (25) can be carried out analytically. Using the average of U [$\bar{U} = U(0)$] and the average of V [$\bar{V} = V(0)$], we get

$$C_Z \rightarrow \rho \omega^2 \bar{U} \quad (28)$$

and

$$C_H \rightarrow \rho g k' \bar{V}. \quad (29)$$

Substituting (28) and (29) in (26) and (27) and using (18) and (20), we get

$$u_z(t) = \frac{1}{4\pi^2} \int_{-\infty}^{\infty} d\mathbf{k} U(\mathbf{k}) \int_{-\infty}^t d\tau \frac{\sin \omega(t-\tau)}{\omega} a(\mathbf{k}') a(-\mathbf{k}') \\ \times \{ -(P_L L_x L_y) \bar{U} \cos(2\omega' \tau) \cos(\mathbf{k} \cdot \mathbf{x}) - (\overline{\Delta P_x} L_x L_y) \bar{V} \cos \Psi \sin(2\omega' \tau) \sin(\mathbf{k} \cdot \mathbf{x}) \} \quad (30)$$

and

$$u_r(t) = \frac{1}{4\pi^2} \int_{-\infty}^{\infty} d\mathbf{k} V(\mathbf{k}) \int_{-\infty}^t d\tau \frac{\sin \omega(t-\tau)}{\omega} a(\mathbf{k}') a(-\mathbf{k}') \\ \times \{ (P_L L_x L_y) \bar{U} \cos(2\omega' \tau) \sin(\mathbf{k} \cdot \mathbf{x}) - (\overline{\Delta P_x} L_x L_y) \bar{V} \cos \Psi \sin(2\omega' \tau) \cos(\mathbf{k} \cdot \mathbf{x}) \}. \quad (31)$$

As we already pointed out in Paper I, the Longuet-Higgins pressure term (P_L) times the source area ($L_x L_y$) is the vertical force and the first terms in (30) and (31) are the wavefields generated by such a vertical force.

The second terms in (30) and (31) show excitation by a horizontal force $\overline{\Delta P_x} L_x L_y$. Proportionality to \bar{V} indicates that they are oscillations excited by a horizontal force. Both terms are accompanied by $\cos \Psi$ which represents the radiation pattern associated with horizontal forcing. This term means that excitation of Rayleigh waves is the maximum in the direction of ocean wave collision and is minimum (zero) in the perpendicular directions.

This term may also be viewed as a dipole, because we can write from (18)

$$-\overline{\Delta P_x} L_x L_y = - \int_{-d}^{\zeta} \frac{\partial(p L_x L_y)}{\partial x} dz \equiv \int_{-d}^{\zeta} \left\{ - \frac{\partial F(z)}{\partial x} \right\} dz, \quad (32)$$

where we defined force $F(z)$ for $p L_x L_y$. This can be interpreted as a horizontal force over an area $L_x L_y$ because it is related to pressure change (p). As the derivative of force with respect to x , $-\partial F(z)/\partial x$, is a dipole source aligned in the x -direction, this term means a horizontal dipole force integrated over the depths of ocean (Fig. 2). The second terms in (30) and (31) are the results of excitation by such dipole forces.

5 DISCUSSION

5.1 Relative size between C_Z and C_H

To examine the importance of horizontal dipoles, we computed C_Z and C_H for PREM-like models but with different ocean depths. Fig. 3 shows the numerical results for six different models; the models have ocean depths 0.5 km (red solid), 1 km (red dash),

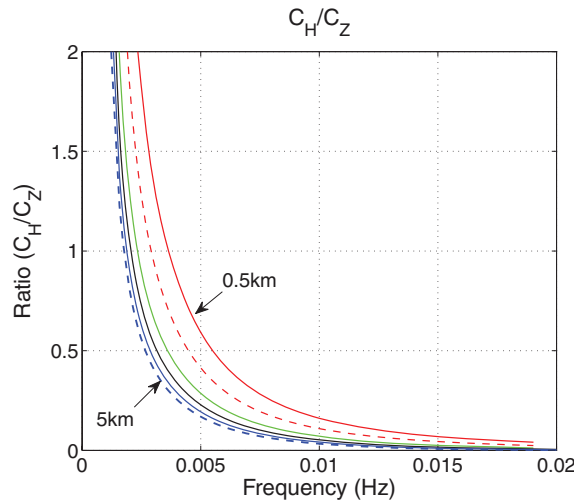


Figure 4. Relative ratio C_H/C_Z . This value becomes larger than 1 for frequencies below about 1–4 mHz. They vary with ocean depths to some extent.

2 km (green), 3 km (black), 4 km (blue solid) and 5 km (blue dash). Density, P - and S -wave velocities are the same with the model PREM.

As our computations were done with dimensional quantities, absolute numbers in the ordinate in Fig. 3 are hard to interpret. Rather, the important points in this figure are in relative amplitudes between C_Z and C_H .

Above 0.05 Hz, it is safe to say that C_Z is about two to three orders of magnitude larger than C_H for any ocean depth and thus is the dominant term for seismic noise. Therefore, in the microseismic frequency band (0.05–0.4 Hz), the pressure effect by the Longuet-Higgins mechanism plays the main role and the horizontal dipole may be ignored.

At low frequencies, the situation changes to some extent. In particular, below 0.005 Hz, amplitudes of C_H can become larger than those of C_Z . Fig. 4 shows the ratio between these quantities (C_H/C_Z) for the frequency range 0–0.2 Hz. To see the cross-over frequencies (when $C_Z = C_H$), only the range for the ratio between 0 and 2 are shown. For any depth of ocean, C_H eventually becomes larger than C_Z at a sufficiently low frequency; it occurs at about 0.003–0.004 Hz for relatively shallow ocean depths (0.5–1 km) and somewhat lower frequencies for deeper oceans. Further discussion on this point as to its cause is given in Section 5.3.

The importance of this term at low frequencies suggests that the excitation of the hum (Kobayashi & Nishida 1998; Suda *et al.* 1998; Tanimoto *et al.* 1998; Rhie & Romanowicz 2004; Tanimoto 2005) may be relevant to this horizontal dipole force, as Webb (2007) proposed. However this relation is not yet established firmly.

5.2 Depth dependence

Fig. 5 shows C_H between 0 and 0.02 Hz. Same colour scheme with Figs 3 and 4 is used to indicate the ocean depths for each curve.

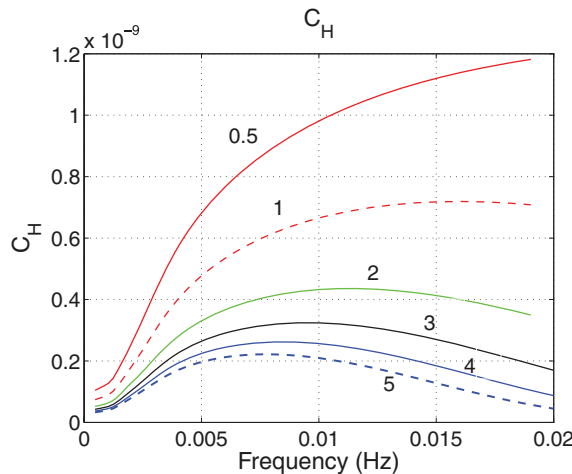


Figure 5. Enlarged plot for C_H for frequencies between 0 and 0.02 Hz. Excitation is more efficient for shallow ocean, although the differences are only factors of 5–10.

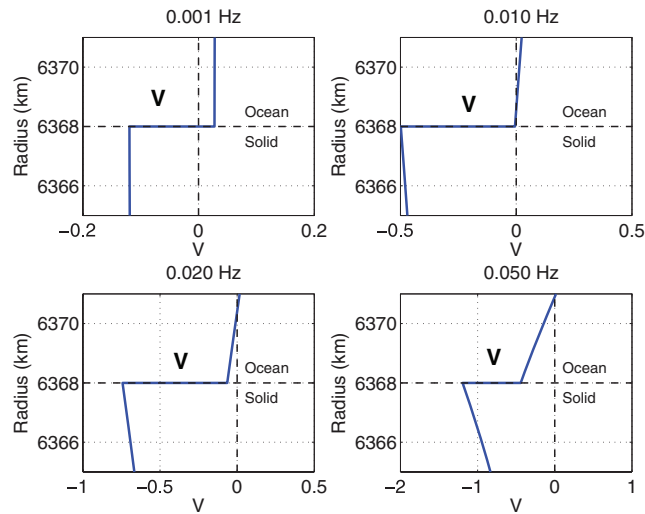


Figure 6. Horizontal eigenfunction V of Rayleigh waves (spheroidal modes). In the oceanic layer of PREM (radius 6368–6371 km), V changes its sign at frequencies about 0.02–0.05 Hz. When V is near zero, it leads to a minimum in the curves for C_H in Fig. 3 at about 0.02–0.05 Hz.

Variations from ocean depths, measured by the differences among 0.5–5 km, are about a factor of five at 0.01 Hz and increase for higher frequencies. Excitation of seismic signals are better for shallower ocean depths. However, differences of factors of five or even ten for this term may be compensated by the area of oceans for each depth range, as the area for ocean depths 4–5 km is quite large in comparison to shallow, continental shelf area. Therefore, this result does not necessarily mean that shallow areas are the likely source of seismic noise in this frequency band.

5.3 Low frequency peak in C_H

In Fig. 3, curves for C_H show curious minimum at frequencies about 0.03–0.05 Hz with secondary peak at about 0.01 Hz. And existence of this secondary peak is closely related to the reason why C_H exceeds C_Z in the low frequency range. However why does C_H show such behaviours?

There are two important features in C_H that bring out this behaviour. One is the fact that the integration part of C_H , in eq. (25), is proportional to B_k^2 , whereas C_Z 's is only linearly proportional. B_k is the horizontal displacement (eigenfunction) of ocean waves. At low frequencies, horizontal displacement becomes dominant for ocean waves, as we know from tsunami waves (shallow-water waves). Fig. 1 shows relative size of vertical and horizontal eigenfunction of ocean-wave modes which clearly demonstrate the dominance of horizontal motion at 3.34 mHz. At a lower frequency, say at 1 mHz, the amplitude of horizontal motion is about an order of magnitude larger than vertical motion. Therefore, in comparison to vertical excitation C_Z , C_H becomes relatively large and eventually exceeds C_Z .

The second important feature in C_H is its proportionality to Rayleigh-wave horizontal eigenfunction $V(z)$. In Fig. 6, we show the behaviours of V for Rayleigh waves (spheroidal modes) in the oceanic layer of PREM. In this figure the top 3 km is the ocean and elastic structure starts at 6368 km (downward). Note that V in the oceanic layer is negative for high frequency Rayleigh-wave modes (0.02 and 0.05 Hz) whereas V is near zero at 0.01 Hz and is positive at 0.001 Hz. Since vertical eigenfunction U is always positive, this means that particle motion in the oceanic layer becomes retrograde to prograde from high frequency to low frequency. This switch-over of sign occurs slightly above 0.01 Hz. The reason that C_H has a minimum in Fig. 3 is related to this behaviour. In other words, as V crosses zero, C_H reaches minimum.

These two features basically explain the cause of secondary peaks of C_H at low frequencies.

5.4 Stokes' drift

It is well known that when we focus on a fluid element in motion, there is a secular drift of fluid element in the direction of wave motion. Linear terms are free from such an effect but there is a secular drift in higher order terms. This phenomenon is included in our analysis as we analyse terms up to the second order. Let us take an example of mass transfer in the x -direction. We consider the transfer of the whole column of mass in the ocean ($-d \leq z \leq \zeta$) and write its transfer in the x -direction as

$$M = \int_{-d}^{\zeta} \rho u \, dz, \quad (33)$$

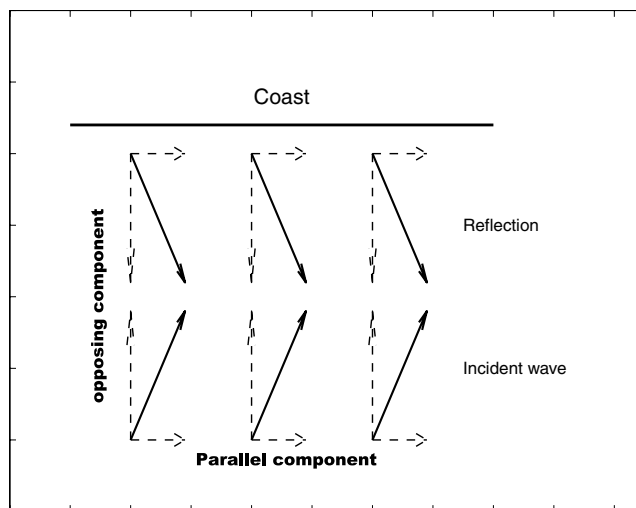


Figure 7. Oblique collision between incoming ocean waves and their reflected waves from the coast. Opposing components lead to the double-frequency terms that are dominant in forces. Parallel components generate static (zero-frequency), non-zero terms. The latter lead to secular transfer of some physical quantities (similar to Stokes' drift).

where u is the x component of velocity. Using basically the same analysis to eq. (16) (Appendix), we get the next formula from (33)

$$\overline{M} = \int d\mathbf{k}' \frac{\rho g k'_x}{2\omega'} \{a^2(\mathbf{k}') - a(\mathbf{k}')a(-\mathbf{k}') \cos(2\omega't)\}, \quad (34)$$

where \overline{M} contains spatial averaging. If we further apply time averaging to this formula, the second term disappears because long-time averaging of cosine term is zero. We are left with

$$\overline{\overline{M}} = \int d\mathbf{k}' \frac{\rho g k'_x}{2\omega'} a^2(\mathbf{k}'), \quad (35)$$

where $\overline{\overline{M}}$ indicates time and spatial averaging.

Physically this term shows the net mass transfer in the x -direction. Over a long time, this leads to secular drift of fluid mass in the direction of wave motion.

This drift, however, does not have any effects on the forces we described in this paper. Note that this is a static term and the main forces in our discussion are the double frequency terms. Secular drift terms, and related terms to them, always show up as static zero-frequency terms in our analysis.

One may say that two opposing waves have same drift terms with opposite signs, and thus there does not exist any secular drift for colliding ocean waves. However, there might be a situation when such drift terms may have relevance to wave-wave interactions; Fig. 7 shows a simple illustration of interaction between incoming ocean waves and their reflections from the coast. They meet in general in oblique angles. Oblique collision means that there are vectorial components that are in the opposite directions, which are the subject of main discussion in this paper, but there are components that are parallel to each other (also parallel to the coast). If we apply our analysis to these parallel waves, there are zero-frequency terms that become important. They are obviously not related to the force equivalents that we discuss in this paper, but they may have relevance to some observations. However further analysis is required to examine the implications of such drift terms.

6 CONCLUSION

When opposing ocean waves collide, there arises not only a vertical force due to the Longuet-Higgins (1950) but also a horizontal dipole force. Its origin was shown, starting from the Navier–Stokes equation. This horizontal force term was already noted in previous publications, but its source was not clear. This term becomes important for the processes below frequency 0.005 Hz because of the dominant horizontal motion of low-frequency ocean waves that are squarely proportional to the excitation coefficient. This horizontal dipole is not likely to be of any significance in the microseismic frequency range (0.05–0.4 Hz), but it may be relevant for the excitation of the hum. It is important to note that both vertical pressure and horizontal dipoles do not generate toroidal-type motions. Explanation of toroidal hums and Love waves in seismic noise thus require an alternative excitation mechanism.

ACKNOWLEDGMENTS

This study was partly supported by the Southern California Earthquake Center (SCEC). SCEC is funded by NSF Cooperative Agreement EAR-0106924 and USGS Cooperative Agreement 02HQAG0008. The SCEC contribution number for this paper is 1331.

REFERENCES

- Dziewonski, A.M. & Anderson, D.L., 1981. Preliminary Reference Earth Model, *Phys. Earth planet. Int.*, **25**, 297–356.
- Hasselmann, K.A., 1963. A statistical analysis of the generation of microseisms, *Rev. Geophys.*, **1**, 177–209.
- Kurrlle, D. & Widmer-Schmidrig, R., 2008. The horizontal hum of the Earth: a global background of spheroidal and toroidal modes, *Geophys. Res. Lett.*, **35**, L06304, doi:10.1029/2007GL033125.
- Kobayashi, N. & Nishida, K., 1998. Continuous excitation of planetary free oscillations by atmospheric disturbances, *Nature*, **395**, 357–360.
- Longuet-Higgins, M.S., 1950. A theory of the origin of microseisms, *Phil. Trans. R. Soc. Lond., Ser. A*, **243**, 1–35.
- Phillips, O.M., 1977. *The Dynamics of the Upper Ocean*, 2nd edn, Cambridge University Press, Cambridge.
- Rhie, J. & Romanowicz, B., 2004. Excitation of Earth's continuous free oscillations by atmosphere-ocean-seafloor coupling, *Nature*, **431**, 552–556.
- Suda, N., Nawa, K. & Fukao, Y., 1998. Earth's background free oscillations, *Science*, **279**, 2089–2091.
- Tanimoto, T., 2005. The oceanic excitation hypothesis for the continuous oscillations of the Earth, *Geophys. J. Int.*, **160**, 276–288.
- Tanimoto, T., 2007. Excitation of normal modes by non-linear interaction of ocean waves, *Geophys. J. Int.*, **168**, 571–582.
- Tanimoto, T., Um, J., Nishida, K. & Kobayashi, N., 1998. Earth's continuous oscillations observed seismically quiet days, *Geophys. Res. Lett.*, **25**, 1553–1556.
- Webb, S.C., 2007. The Earth hum is driven by ocean waves over the continental shelves, *Nature*, **445**, 754–756.
- Webb, S.C., 2009. The Earth's hum: the excitation of Earth normal modes by ocean waves, *Geophys. J. Int.*, **174**, 542–566.

APPENDIX

Derivation of (16)

Time derivative of the x -component of velocity u can be written from (8) to (11)

$$\begin{aligned} \frac{\partial u}{\partial t} &= \int B_{k'} \frac{k'_x \omega'}{k'} a(\mathbf{k}') \cos(\omega' t - \mathbf{k}' \cdot \mathbf{x}) d\mathbf{k}' \\ &= \int \frac{\cosh\{k'(z+d)\}}{\sinh(k'd)} \frac{k'_x \omega'^2}{k'} a(\mathbf{k}') \cos(\omega' t - \mathbf{k}' \cdot \mathbf{x}) d\mathbf{k}'. \end{aligned} \quad (\text{A1})$$

The dispersion relation like (7) holds between ω' and \mathbf{k}' . The integration over the depth of ocean can be carried out analytically

$$\rho \int_{-d}^{\zeta} \frac{\partial u}{\partial t} dz = \rho \int \frac{\sinh\{k'(\zeta+d)\}}{\sinh(k'd)} \frac{k'_x \omega'^2}{k'^2} a(\mathbf{k}') \cos(\omega' t - \mathbf{k}' \cdot \mathbf{x}) d\mathbf{k}'. \quad (\text{A2})$$

The integrand contains one $a(\mathbf{k}')$ but additional higher order terms arise because of ζ which is proportional to $a(\mathbf{k}')$ (see eq. 12). To keep terms up to the second order in ocean-wave amplitudes, we expand

$$\frac{\sinh\{k'(\zeta+d)\}}{\sinh(k'd)} \approx 1 + k'\zeta \frac{\cosh(k'd)}{\sinh(k'd)} \quad (\text{A3})$$

and substitute in the integrand. When spatial averaging is taken, contribution from the leading order term of 1 in this formula disappears. Keeping only the second term in (A3), we get

$$\begin{aligned} \rho \int_{-d}^{\zeta} \frac{\partial u}{\partial t} dz &= \rho \int \zeta \frac{\cosh(k'd)}{\sinh(k'd)} \frac{k'_x \omega'^2}{k'} a(\mathbf{k}') \cos(\omega' t - \mathbf{k}' \cdot \mathbf{x}) d\mathbf{k}' \\ &= \int \rho g k'_x \zeta a(\mathbf{k}') \cos(\omega' t - \mathbf{k}' \cdot \mathbf{x}) d\mathbf{k}', \end{aligned} \quad (\text{A4})$$

where we used the dispersion relation $\omega'^2 = gk' \tanh(k'd)$. Substituting

$$\zeta = \int d\mathbf{k}'' a(\mathbf{k}'') \sin(\omega'' t - \mathbf{k}'' \cdot \mathbf{x}) \quad (\text{A5})$$

we get

$$\begin{aligned} \rho \int_{-d}^{\zeta} \frac{\partial u}{\partial t} dz &= \int d\mathbf{k}' \int d\mathbf{k}'' \rho g k'_x a(\mathbf{k}') a(\mathbf{k}'') \cos(\omega' t - \mathbf{k}' \cdot \mathbf{x}) \sin(\omega'' t - \mathbf{k}'' \cdot \mathbf{x}) \\ &= \int d\mathbf{k}' \int d\mathbf{k}'' \frac{\rho g k'_x}{2} a(\mathbf{k}') a(\mathbf{k}'') \\ &\quad \times [\sin\{(\omega' + \omega'')t - (\mathbf{k}' + \mathbf{k}'') \cdot \mathbf{x}\} - \sin\{(\omega' - \omega'')t - (\mathbf{k}' - \mathbf{k}'') \cdot \mathbf{x}\}]. \end{aligned} \quad (\text{A6})$$

When spatial averaging is taken, the first sine term in this formula gives contribution at $\omega'' = \omega'$ and $\mathbf{k}'' = -\mathbf{k}'$. The second sine term should make contribution at $\omega'' = \omega'$ and $\mathbf{k}'' = \mathbf{k}'$ but because this is a sine term, it identically vanishes when these conditions are met. Then, we get the eq. (16)

$$\rho \int_{-d}^{\zeta} \frac{\partial u}{\partial t} dz = \int d\mathbf{k}' \frac{\rho g k'_x}{2} a(\mathbf{k}') a(-\mathbf{k}') \sin(2\omega' t). \quad (\text{A7})$$

Derivation of (17)

Using a similar analysis to (16), we can get

$$\int_{-d}^{\zeta} \rho u \frac{\partial u}{\partial x} dz = \int_{-d}^{\zeta} dz \int d\mathbf{k}' \frac{\rho}{2} a(\mathbf{k}') a(-\mathbf{k}') B_{k'}^2 \frac{k_x'^3}{k'^2} \sin(2\omega't) \quad (\text{A8})$$

$$\int_{-d}^{\zeta} \rho v \frac{\partial u}{\partial y} dz = \int_{-d}^{\zeta} dz \int d\mathbf{k}' \frac{\rho}{2} a(\mathbf{k}') a(-\mathbf{k}') B_{k'}^2 \frac{k_x' k_y'^2}{k'^2} \sin(2\omega't) \quad (\text{A9})$$

$$\int_{-d}^{\zeta} \rho u \frac{\partial u}{\partial x} dz = \int_{-d}^{\zeta} dz \int d\mathbf{k}' \frac{\rho}{2} a(\mathbf{k}') a(-\mathbf{k}') A_{k'}^2 k_x' \sin(2\omega't). \quad (\text{A10})$$

Therefore,

$$\int_{-d}^{\zeta} \rho \left(u \frac{\partial u}{\partial x} + v \frac{\partial u}{\partial y} + w \frac{\partial u}{\partial z} \right) dz = \int_{-d}^{\zeta} dz \int d\mathbf{k}' \frac{\rho}{2} a(\mathbf{k}') a(-\mathbf{k}') (A_{k'}^2 + B_{k'}^2) k_x' \sin(2\omega't). \quad (\text{A11})$$

The integration over z can be analytically carried out because the only functions of z are $A_{k'}$ and $B_{k'}$. We get

$$\int_{-d}^{\zeta} (A_{k'}^2 + B_{k'}^2) dz = \frac{\omega'^2 \sinh\{2k'(\zeta + d)\}}{2k' \sinh^2(k'd)}. \quad (\text{A12})$$

The integrand in the formula (A11) already contains two amplitude terms $a(\mathbf{k}') a(-\mathbf{k}')$. Therefore, the contribution from ζ in (A12) leads to third-order terms at the highest. We thus drop ζ in (A12). It is now easy to show, using the dispersion relation,

$$\int_{-d}^{\zeta} (A_{k'}^2 + B_{k'}^2) dz = \frac{\omega'^2 \cosh(k'd)}{k' \sinh(k'd)} = g. \quad (\text{A13})$$

Substitution in (A11) leads us to the eq. (17)

$$\int_{-d}^{\zeta} \rho \left(u \frac{\partial u}{\partial x} + v \frac{\partial u}{\partial y} + w \frac{\partial u}{\partial z} \right) dz = \int d\mathbf{k}' \frac{\rho g k_x'}{2} a(\mathbf{k}') a(-\mathbf{k}') \sin(2\omega't). \quad (\text{A14})$$